Dalton Transactions

Novel N6 trisbidentate ligand coordinated Ir(III) complexes and their Ru(II) analogs

Journal:	*Dalton Transactions*
Manuscript ID	DT-COM-09-2018-003544.R1
Article Type:	Communication
Date Submitted by the Author:	15-Sep-2018
Complete List of Authors:	Wang, Li; North Dakota State University, Chemistry; Houston Methodist Hospital, Cui, Peng; Rutgers The State University of New Jersey, Materials science and engineering Liu, Bingqing; North Dakota State University, Kilina, Svetlana; North Dakota State University, Chemistry and Biochemistry Sun, Wenfang; North Dakota State University, Chemistry

Dalton Transactions

COMMUNICATION

Novel N_6 trisbidentate ligand coordinated Ir(III) complexes and their Ru(II) analogs

Received 00th January 20xx,
Accepted 00th January 20xx

DOI: 10.1039/x0xx00000x

www.rsc.org/

Li Wang,[a] Peng Cui,[a,b] Bingqing Liu,[a] Svetlana Kilina[a] and Wenfang Sun[a,*]

Novel N_6-coordinated Ir(III) complexes bearing polypyridyl ligands were synthesized and characterized. In comparison to their Ru(II) analogs, these Ir(III) complexes showed blue-shifted UV-vis absorption and emission spectra, but dramatically increased triplet lifetimes with much broader and stronger triplet excited-state absorption.

After the seminal work by Watts et al. in the 1980s,[1] investigations on luminescent iridium(III) complexes have attracted a great attention over the past few decades.[2-4] Iridium is known to have strong spin-orbit coupling constants (3909 cm^{-1});[5] thus, it can facilitate intersystem crossing to greatly populate the triplet excited state in the formed complexes. The energies of the emissive triplet excited states of the complexes can be readily tuned by modification of the coordination sphere; therefore, emission colours of the Ir(III) complexes can cover the entire visible spectral range.[6-8] Due to these characteristics, Ir(III) complexes have become the most attractive class of phosphorescent heavy-metal complexes and have been widely used in organic light-emitting diodes (OLED),[3,9] light-emitting electrochemical cells (LEEC),[10,11] biolabeling,[12,13] and chemosensors.[14,15]

To date, four types of iridium complexes with tris-bidentate ligands have been reported in literature, *i.e.*, triscyclometalated iridium complexes $Ir(C^N)_3$,[16,17] biscyclometalated complexes $[Ir(C^N)_2(N^N)]^+$,[10,12,15] monocyclometalated complexes $[Ir(C^N)(N^N)_2]^{2+}$,[18] and N_6-coordinated $[Ir(N^N)_3]^{3+}$ complexes[18-22] (where C^N refers to cyclometalating ligands and N^N refers to diimine ligands), with $Ir(C^N)_3$ and $[Ir(C^N)_2(N^N)]^+$ complexes being those most studied. In contrast, heteroleptic $[Ir(N^N)_2(N^N)']^{3+}$ complexes have been rarely investigated,[18-22] presumably due to the lack of effective synthetic routes and an intractable purification process.[23-25]

Compared to the well-studied cyclometalated iridium complexes,[1-17] N_6-coordinated Ir(III) complexes bearing polypyridyl ligands exhibited different photophysical properties and showed better inherent water solubility due to the increased number of positive charges, which is a desirable feature for biological applications of this class of complexes. Recently, Stimpson et al. reported a new N_6-coordinated Ir(III) complex with two bipyridine ligands and one dipyridophenazine (**dppz**) ligand. In addition to the expected good water solubility, this complex featured a ligand-centered $^3\pi,\pi^*$ emitting state and DNA affinity that was comparable to its Ru(II) analogue.[18]

Due to the challenge of synthesizing $[Ir(N^N)_3]^{3+}$ complexes, limited photophysical study has been reported for these types of complexes despite their potential biological applications.[18-22] To the best of our knowledge, no structure-property correlation has ever been reported for this class of complexes. In our research, we synthesized and investigated two complexes ($[Ir(N^N)_3]^{3+}$ and $[Ir(N^N)_2(N^N)']^{3+}$) based on phenanthroline or substituted phenanthroline ligand(s) (structure shown in Chart 1). Their corresponding Ru(II) analogues were synthesized and studied as well in order to understand the effect of the ligand π-conjugation and the metal centre on the photophysics of the complexes.

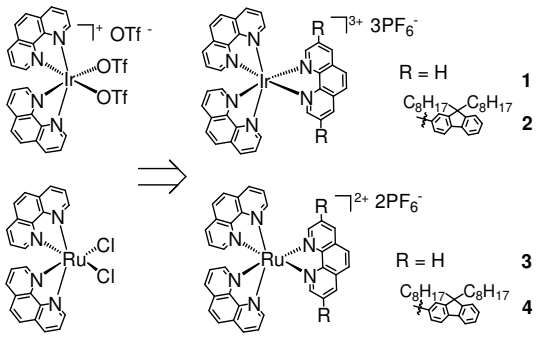

Chart 1 Chemical structures of the target Ir(III) and Ru(II) complexes and their precursors.

To prepare the Ir(III) complexes, $[Ir(phen)_2Cl_2]PF_6$ was first synthesized by refluxing phenanthroline and $IrCl_3$ hydrates in glycerol; then, the inert chloride ligands were changed to $CF_3SO_3^-$ ligands by reacting with CF_3SO_3H according to Meyer's

[a] Department of Chemistry and Biochemistry, North Dakota State University, Fargo, North Dakota, 58108-6050, USA.
[b] Materials and Nanotechnology Program, North Dakota State University, Fargo, North Dakota, 58108, USA.

† Electronic supplementary information (ESI) available. See DOI:10.1039/x0xx00000x

method.[26] The target Ir(III) complexes **1** and **2** were then readily prepared by refluxing $[Ir(phen)_2(OTf)_2]OTf$ and the third diimine ligand in 1,2-dichlorobenzene. The synthesis of the *cis*-$(phen)_2RuCl_2{\cdot}xH_2O$ precursor was conducted by a reaction of phenanthroline and $RuCl_3$ hydrates in refluxed anhydrous dimethylformamide (DMF) as described in the literature.[27] During the reaction, the Ru(III) ion was reduced to Ru(II) by the volatile dimethylamine that was generated in situ *via* DMF decomposition at its boiling temparature. The two target Ru(II) complexes **3** and **4** were then synthesized by refluxing the *cis*-$(phen)_2RuCl_2{\bullet}xH_2O$ precursor with the corresponding diimine ligands in ethanol. The structures of complexes **1-4** were characterized by ^{1}H NMR, HRMS and elemental analysis (ESI Figs. S1-S4).

The UV-vis absorption and steady-state emission of the four complexes were studied in acetonitrile solutions (Fig. 1), and the related data are presented in Table 1. The obedience of absorption to Beer's Law in the studied concentration range (5×10^{-6} to 1×10^{-4} mol·L^{-1}, ESI Fig. S5) indicates the absence of ground-state aggregation. However, the low-energy absorption band(s) of the Ir(III) complexes were blue-shifted compared to those of their Ru(II) analogues. A similar phenomenon was observed in the bis-tridentate Ir(III) and Ru(II) complexes.[28] Introducing fluorenyl substituents to one of the phenanthroline ligands gave rise to an additional broad band at ca. 420 nm for complex **2** (compared to complex **1**), and at ca. 380 nm for complex **4** (compared to complex **3**). Meanwhile, the lowest energy absorption band, *i.e.,* the metal-to-ligand charge transfer (^{1}MLCT) bands[29,30] of **3**, was slightly red-shifted compared to that of **4**.

The emission spectrum of **1** appeared between 420 and 600 nm with a clear vibronic structure, indicative of a ligand-based $^3\pi,\pi^*$ emission.[18] In contrast, the emission spectra of **2**, **3**, and **4** were much less structured and in the red region, suggesting a significant charge transfer nature in the emission. The emission quantum yield of **1** was higher than that of **2**, which is in line with a predominant $^3\pi,\pi^*$ emission. In contrast, despite the fact that the emission of **4** was slightly red-shifted (~15 nm) compared to that of **3**, the emission lifetime of **4** (1.41 μs) was much longer than that of **3** (0.39 μs), and it was accompanied by an increased emission quantum yield. A comparison of the UV-vis absorption and emission spectra of **2** and **4** to those of **1** and **3**, respectively, revealed that the introduction of fluorenyl substituents caused a significant change in both the absorption and emission spectra of **2** and **4**. However, the impacts of the fluorenyl substitution on the Ir(III) complexes are more dramatic than those on the Ru(II) complexes.

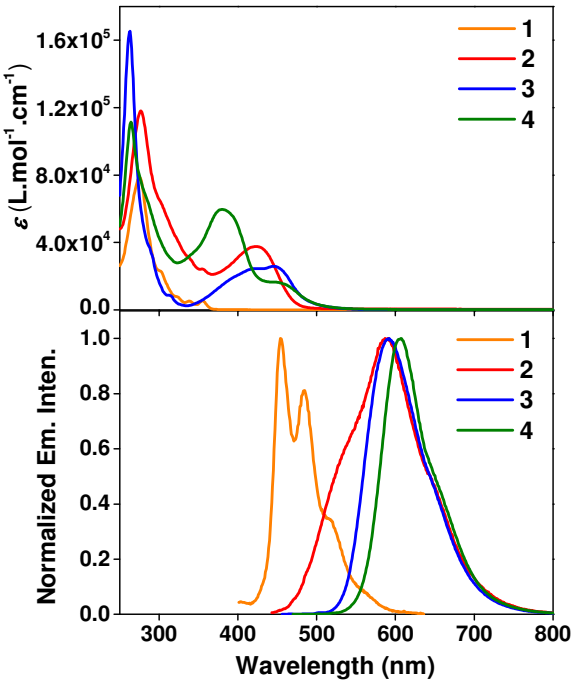

Fig. 1 UV-vis absorption (top) and emission (bottom) spectra of **1-4** in acetonitrile at room temperature.

Table 1 Photophysical data for complexes **1-4** in acetonitrile at room temperature

	λ_{abs}/nm (ε/10^4 L mol^{-1} cm^{-1})[a]	λ_{em}/nm (τ/μs); Φ_{em}[b]	$^{theor}\lambda_{phos}$/nm[c]	$\lambda_{T1\text{-}Tn}$/nm (τ_T/μs; $\varepsilon_{T1\text{-}Tn}$/10^4 L mol^{-1} cm^{-1}); Φ_T[d]
1	276 (5.09), 304 (1.47), 325 (0.48), 340 (0.32), 354 (0.36)	455 (4.16), 485 (4.17), 520 (4.12); 0.098[e]	452	370 (4.27; -), 590 (4.52; -), 750 (5.08; -); -[f]
2	277 (11.84), 305 (6.11), 354 (2.44), 423 (3.78)	545 (sh., -), 588 (-)[g]; 0.024	562	497 (73.8; 1.33), 720 (80.8; 3.14); 0.77
3	263 (16.52), 290 (3.97), 412 (2.51), 447 (2.64)	590 (0.39); 0.029	562	590 (0.38; 0.66); 1
4	264 (10.87), 383 (5.90), 457 (1.56)	605 (1.41); 0.08	630	443 (1.49; -), 491 (1.39; -), 662 (1.47; 2.37); 0.67

[a] Absorption band maxima and molar extinction coefficients. [b] Emission band maxima, intrinsic lifetimes and emission quantum yields. A degassed $[Ru(bpy)_3]Cl_2$ in acetonitrile solution was used as the reference (λ_{ex} = 436 nm, Φ_{em} = 0.097). [c] Calculated phosphorescence energies using PBE1PBE functional for optimized triplet geometry. [d] Nanosecond transient absorption band maxima, triplet extinction coefficients, triplet excited-state lifetimes and quantum yields. SiNc in C_6H_6 was used as the reference (ε_{590nm} = 70,000 L mol^{-1} cm^{-1}, Φ_{em} = 0.20). [e] 1 N sulfuric acid solution of quinine bisulfate (λ_{ex} = 347.5 nm, Φ_{em} = 0.546) was used as the reference. [f] No bleaching was observed, thus the $\varepsilon_{T1\text{-}Tn}$ and Φ_T cannot be calculated. [g] Emission signal was too weak to allow the lifetime to be measured.

It is worth noting that the emission spectrum of complex **2** possessed a shoulder at ca. 545 nm in addition to the major emission band at 588 nm. Although the nature of these two bands could not be distinguished based on their respective lifetimes, which could not be determined for either band due to the very weak emission signals, measurements in air-saturated CH_3CN solution and deaerated solution clearly manifested their different

natures. As displayed in Fig. 2, the 545 nm shoulder in the emission spectrum of **2** was not subjected to be quenched by oxygen, but the 588 nm band was essentially quenched in the presence of oxygen. This implies a fluorescence nature for the 545 nm shoulder and a phosphorescence nature for the 588 nm band. The excitation spectrum monitored at 545 nm emission (ESI Fig. S7) matched the 423 nm charge transfer band in its UV-vis absorption spectrum. Additionally, both the shape and energy of the 545 nm band resembled the intraligand charge transfer (ILCT, a charge transfer transition from a π orbital localized on one component of a ligand to a π^* orbital based on another component of the same ligand. It refers to the π(fluorenyl)$\rightarrow\pi^*$(phen) transition in this work.) fluorescence from the $ZnCl_2$ coordinated fluorenyl substituted phen ligand (ESI Fig. S8). All this experimental evidence suggests the ^{1}ILCT fluorescence nature for the 545 nm shoulder.

To better understand the aforementioned differences and unambiguously identify the electronic transitions contributing to the observed absorption and emission, time-dependent density functional theory (TDDFT) calculations were carried out for complexes **1-4**. The ground-state MOs and energy diagrams are presented in Fig. 3, and the natural transition orbitals (NTOs)[31] or MOs corresponding to the major optical transitions are given in ESI Tables S1-S4. For Ir(III) complex **1**, the low-energy absorption bands were dominated by the ligand-localized $^1\pi,\pi^*$ transitions mixed with some ^{1}MLCT transitions. For complex **2**, its low-energy absorption band had a predominant contribution from the intraligand charge transfer (^{1}ILCT) transition, and the $^1\pi,\pi^*$ transition also made a minor contribution. For Ru(II) complex **3**, the calculation results revealed that the ^{1}MLCT transitions were the exclusive contributors to the low-energy absorption bands. For complex **4**, in addition to the major contributions from the ^{1}MLCT transitions, the ^{1}ILCT/$^1\pi,\pi^*$ transitions based on the substituted phenanthroline ligand made a significant contribution. A comparison of the natures of the low-energy absorption bands in the Ir(III) complexes **1** and **2** to those in the Ru(II) complexes **3** and **4** revealed that the ^{1}MLCT transitions made exclusive or major contributions in the Ru(II) complexes, while the ligand-localized $^1\pi,\pi^*$ or ^{1}ILCT/$^1\pi,\pi^*$ transitions were the dominant contributors in the Ir(III) complexes. However, introducing the fluorenyl substituents on one of the phenanthroline ligands induced a significant/major contribution from the ^{1}ILCT transitions in both the Ir(III) and Ru(II) complexes **2** and **4**.

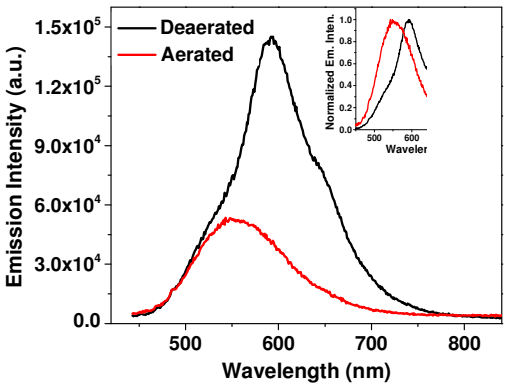

Fig. 2 Emission spectra of complex **2** in air-saturated and degassed CH_3CN solutions. The inset shows the normalized emission spectra in these two conditions. $c = 1\times10^{-5}$ mol.L^{-1}.

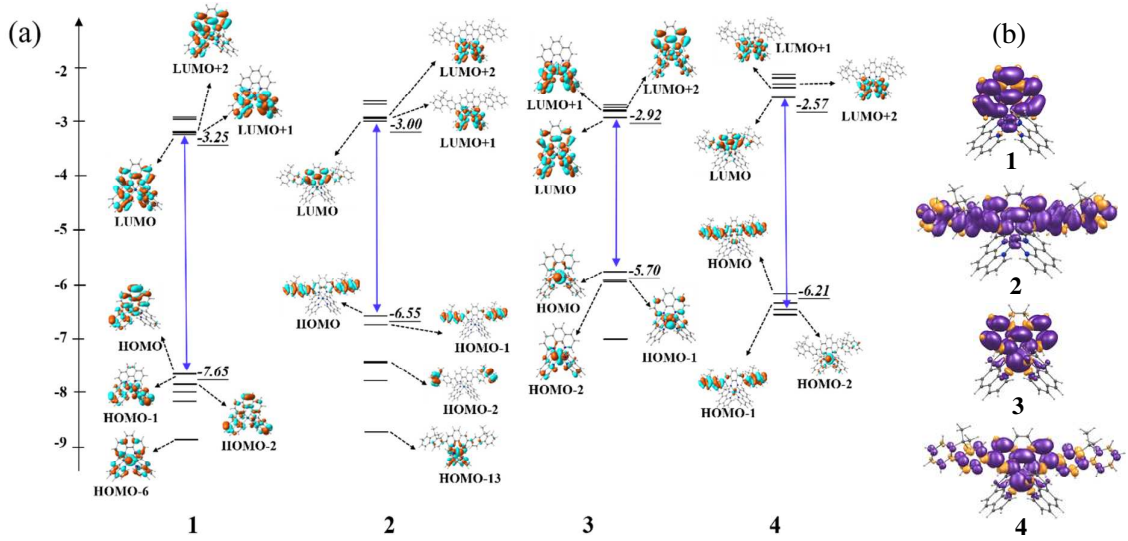

Fig. 3 (a) Schematic diagram showing the MO distributions and their energy levels in complexes **1–4** from DFT calculations. (The blue arrow shows the major contribution to the lowest energy transitions for each complex). (b) Isosurfaces of the spin density of complexes **1**-**4** at the optimized triplet state geometry.

For the triplet emitting states, the DFT calculation results (see the isosurfaces of the spin density distribution in Fig. 3(b) and the major contributing MOs displayed in ESI Table S4) indicated the presence of major $^3\pi,\pi^*$ characters in both **1** and **2**, with a minor ^{3}MLCT character in **1** and **2** and a significant contribution from ^{3}ILCT in **2**. In contrast, the emissions of the two Ru(II) complexes both had mixed $^3\pi,\pi^*/^3$MLCT characters. The MOs contributing to the triplet emitting states of **2** and **4** clearly showed that these emitting states had more charge transfer characters, *i.e.,* more ^{3}ILCT character in **2** and more ^{3}MLCT character in **4** in comparison to the pure $^3\pi,\pi^*$ character in the triplet emitting state of the fluorenyl substituted phen ligand (ESI Table S5). In addition, the unoccupied MOs of **2** and **4** were more localized on the phen motif. Therefore, the emission energies of **2** and **4** were higher than that of the pure $^3\pi,\pi^*$ state from the ligand.

To gain further insight into the dramatic impacts of the metal ions (although both metal ions belong to d^6 transition metals) on the absorption and emission spectral features and into the natures of the lowest singlet and triplet excited states of the Ir(III) and Ru(II) complexes, the crystal field splitting energies (Δ_{oct}) for **1**-**4** were calculated. The calculated Δ_{oct} was 3.76 eV for **1**, 3.95 eV for **2**, 2.46 eV for **3**, and 2.89 eV for **4**. Unsurprisingly, the two Ir(III) complexes had a larger Δ_{oct} compared to the two Ru(II) analogues, and the complexes bearing the fluorenyl substituted phen ligand (*i.e.* **2** and **4**) had a higher Δ_{oct} than their corresponding complexes **1** and **3**. The Ir(III) ion has a higher oxidation state and more electrons than the Ru(II) ion; thus, the Δ_{oct} is larger in Ir(III) complexes than in Ru(II) complexes. The larger splitting stabilizes the t_{2g} orbitals further in the Ir(III) complexes than in the Ru(II) complexes. Consequently, these high-lying, occupied t_{2g} orbitals in Ru(II) complexes were more involved in the frontier molecular orbitals (FMOs) – such as HOMO, HOMO-1, and HOMO-2 – and thus made the MLCT transitions the dominant contributors in the Ru(II) complexes **3** and **4**. In contrast, the deeper t_{2g} orbitals in Ir(III) complexes made minor contributions to the FMOs of these complexes, and MLCT transitions got less involved in the low-energy absorption bands and in the emission of the Ir(III) complexes **1** and **2**. Moreover, when π-donating fluorenyl substituents were introduced in one of the phenanthroline ligands, the ligand field became stronger in **2** and **4**, increasing the Δ_{oct} in these two complexes compared to that in **1** and **3**, respectively. Consequently, the MLCT contributions to the low-energy absorption bands and emission in **2** and **4** were reduced compared to those in **1** and **3**. Therefore, the impact of the metal ions in **2** and **4** became less dramatic than in **1** and **3**, which was reflected by the smaller difference of the Δ_{oct} values between **2** and **4** (1.06 eV) than between **1** and **3** (1.30 eV) and was clearly evidenced by the less marked differences in the absorption and emission spectra of **2** and **4**.

The triplet excited state characteristics of all complexes were further investigated using nanosecond (ns) transient absorption (TA) spectroscopy. The time-resolved TA spectra of these complexes are presented in Fig. 4 and ESI Fig. S10, and the triplet excited-state parameters are compiled in Table 1. The TA spectrum of **1** was quite broad, covering from the entire visible to the near-IR spectral region (360 - 800 nm), and it decayed within 4.5 μs. For complex **2**, the TA spectrum featured a bleaching band at ca 428 nm and broad positive bands from 460 to 800 nm. The transient absorbing triplet excited state was very long-lived, with a lifetime of approximately 81 μs. The position of the bleaching band was consistent with the position of the ^{1}ILCT/$^1\pi,\pi^*$ absorption band in the UV-vis absorption spectrum of **2**. In contrast to the corresponding TA spectra of Ir(III) complexes, the TA spectra of the Ru(II) complexes **3** and **4** were comparably weaker and narrower. Their lifetimes were one to two orders of magnitude shorter than those of their corresponding Ir(III) complexes. Because the lifetimes obtained from the decay of TA signals were consistent with those measured from the decay of emission, it is reasonable to attribute the excited states giving rise to the observed TA to the emitting excited states. Based on the nature of the emitting triplet excited states in the complexes discussed above, it is clear that the lowest triplet excited states (T_1) in the Ru(II) complexes have more ^{3}MLCT character, while those states in the Ir(III) complexes are dominated by the $^3\pi,\pi^*$ character. This difference impacted the lifetimes of the T_1 states in the Ru(II) and Ir(III) complexes dramatically. Another general feature that emerged is that the two complexes bearing the fluorenyl substituted phenanthroline ligand, *i.e.,* **2** and **4**, exhibited stronger TA signals in the visible and near-IR regions and much longer lifetimes compared to the complexes without the fluorenyl substituents on the phen ligand, *i.e.,* **1** and **3**.

In summary, we have synthesized two novel Ir(III) tris-diimine complexes and systematically studied their photophysical properties. The excited-state properties of these complexes were compared to those of their corresponding Ru(II) counterparts with the same set of ligands. Our results have shown that both the metal center and ligand π-conjugation had a significant influence on the ground-state and excited-state absorption, emission, and triplet lifetimes. Due to the higher oxidation state and greater number of electrons in the Ir(III) ion compared to the Ru(II) ion, the crystal field splitting energies of the d orbitals in Ir(III) complexes were much larger than those in the corresponding Ru(II) complexes. Thus, the d orbitals in the Ir(III) complexes are more deeply situated and do not significantly contribute to the frontier molecular orbitals of these complexes compared to their Ru(II) analogues.

Consequently, their lowest singlet and triplet excited states characteristics mainly reflected the ligand-localized π,π^* excited states in contrast to the dominant MLCT characters in the Ru(II) complexes. This led to much longer-lived triplet excited states in the Ir(III) complexes, and the impact of extended π-conjugation in the ligand became more distinct in these complexes. The long-lived triplet excited states and the broad and strong triplet excited-state absorption in these Ir(III) complexes make them excellent candidates as potential reverse saturable absorbers for optical limiting applications and as photosensitizers for photodynamic therapy applications. These studies will be carried out in the near future.

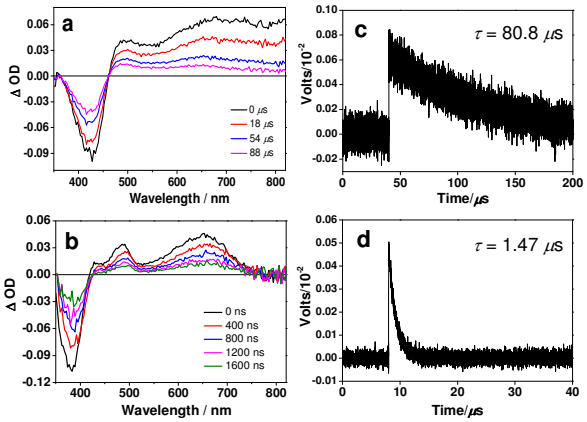

Fig. 4 Time-resolved TA spectra of **2** (a) and **4** (b) and the decay curves at the corresponding TA maxima, *i.e.* 720 nm for **2** (c) and 660 nm for **4** (d) in acetonitrile at room temperature. λ_{ex} = 355 nm, A_{355} = 0.4 in a 1-cm cuvette.

This work was partially supported by National Science Foundation (DMR-1411086), the Sloan Foundation (Research Fellowship BR2014-073), and the U.S. Department of Energy Early-Career Grant DESC008446.

Conflicts of interest

There are no conflicts to declare.

Notes and references

1 K. A. King, P. J. Spellane and R. J. Watts, *J. Am. Chem. Soc.*, 1985, **107**, 1431-1432.
2 K. K.-W. Lo, *Acc. Chem. Res.*, 2015, **48**, 2985-2995.
3 X. Yang, G. Zhou and W.-Y. Wong, *Chem. Soc. Rev.*, 2015, **44**, 8484-8575.
4 J. A. G. Williams, A. J. Wilkinson and V. L. Whittle, *Dalton Trans.*, 2008, 2081-2099.
5 G. Zhang, H. Zhang, Y. Gao, R. Tao, L. Xin, J. Yi, F. Li, W. Liu and J. Qiao, *Organometallics*, 2014, **33**, 61-68.
6 T. Tsuzuki, N. Shirasawa, T. Suzuki and S. Tokito, *Adv. Mater.*, 2003, **15**, 1455-1458.
7 T. Hu, L. He, L. Duan and Y. Qiu, *J. Mater. Chem.*, 2012, **22**, 4206-4215.
8 Q. Zhao, M. Yu, L. Shi, S. Liu, C. Li, M. Shi, Z. Zhou, C. Huang and F. Li, *Organometallics*, 2010, **29**, 1085-1091.
9 M. S. Lowry and S. Bernhard, *Chem. Eur. J.*, 2006, **12**, 7970-7977.
10 R. D. Costa, E. Ortí, H. J. Bolink, F. Monti, G. Accorsi and N. Armaroli, *Angew. Chem. Int. Ed.*, 2012, **51**, 8178-8211.
11 Z. Liu, W. Qi and G. Xu, *Chem. Soc. Rev.*, 2015, **44**, 3117-3142.
12 V. Fernandez-Moreira, F. L. Thorp-Greenwood and M. P. Coogan, *Chem. Commun.*, 2010, **46**, 186-202.
13 Y. Yang, Q. Zhao, W. Feng and F. Li, *Chem. Rev.*, 2013, **113**, 192-270.
14 Q. Zhao, F. Li and C. Huang, *Chem. Soc. Rev.*, 2010, **39**, 3007-3030.
15 Z. Mao, M. Wang, J. Liu, L.-J. Liu, S. M.-Y. Lee, C.-H. Leung and D.-L. Ma, *Chem. Commun.*, 2016, **52**, 4450-4453.
16 A. B. Tamayo, B. D. Alleyne, P. I. Djurovich, S. Lamansky, I. Tsyba, N. N. Ho, R. Bau and M. E. Thompson, *J. Am. Chem. Soc.*, 2003, **125**, 7377-7387.
17 A. Tsuboyama, H. Iwawaki, M. Furugori, T. Mukaide, J. Kamatani, S. Igawa, T. Moriyama, S. Miura, T. Takiguchi, S. Okada, M. Hoshino and K. Ueno, *J. Am. Chem. Soc.*, 2003, **125**, 12971-12979.
18 S. Stimpson, D. R. Jenkinson, A. Sadler, M. Latham, D. A. Wragg, A. J. H. M. Meijer and J. A. Thomas, *Angew. Chem. Int. Ed.*, 2015, **54**, 3000-3003.
19 M. Pandrala, F. Li, L. Wallace, P. J. Steel, B. Moore II, J. Autschbach, J. G. Collins and F. R. Keene, *Aust. J. Chem.*, 2013, **66**, 1065-1073.
20 S. Soman, J. C. Manton, J. L. Inglis, Y. Halpin, B. Twamley, E. Otten, W. R. Browne, L. De Cola, J. G. Vos and M. T. Pryce, *Chem. Commun.*, 2014, **50**, 6461-6463.
21 E. Krausz, J. Higgins and H. Riesen, *Inorg. Chem.*, 1993, **32**, 4053-4056.
22 N. P. Ayala, C. M. Flynn, Jr., L. Sacksteder, J. N. Demas and B. A. Degraff, *J. Am. Chem. Soc.*, 1990, **112**, 3837-3844.
23 R. J. Watts, J. S. Harrington and J. Van Houten, *J. Am. Chem. Soc.*, 1977, **99**, 2179-2187.
24 W. A. Wickramasinghe, P. H. Bird and N. Serpone, *J. Chem. Soc., Chem. Commun.*, 1981, 1284-1286.
25 G. Nord, A. C. Hazell, R. G. Hazell and O. Farver, *Inorg. Chem.*, 1983, **22**, 3429-3434.
26 B. P. Sullivan and T. J. Meyer, *J. Chem. Soc., Chem. Commun.*, 1984, 403-405.
27 C. Viala and C. Coudret, *Inorg. Chim. Acta.*, 2006, **359**, 984-989.
28 M. Cavazzini, P. Pastorelli, S. Quici, F. Loiseau and S. Campagna, *Chem. Commun.*, 2005, 5266-5268.
29 J. F. Endicott, H. B. Schlegel, M. J. Uddin and D. S. Seniveratne, *Coord. Chem. Rev.*, 2002, **229**, 95-106.
30 K. Nakamaru, *Bull. Chem. Soc. Jpn.*, 1982, **55**, 2697-2705.
31 R. L. Martin, *J. Chem. Phys.*, 2003, **118**, 4775-4777.

Dalton Transactions

COMMUNICATION

Table of Contents Entry

N_6-coordinated Ir(III) complexes showed blue-shifted UV-vis absorption and emission, but dramatically long-lived broad and strong triplet excited-state absorption.